



ISSN 0975-413X
CODEN (USA): PCHHAX

Der Pharma Chemica, 2016, 8(1):294-303
(<http://derpharmachemica.com/archive.html>)

Investigation of corrosion inhibition of mild steel in 1M HCl by 3-methyl-4-(3-methyl-isoxazol-5-yl)isoxazol-5(2H)-one monohydrate using experimental and theoretical approaches

S. Lahmidi¹, H. Elmsellem², A. Elyoussfi², N. K. Sebbar¹, E. M. Essassi¹, Y. Ouzidan³, Y. Kandri Rodi³, K. Dguigui⁴, B. El Mahi² and B. Hammouti²

¹Laboratoire de Chimie Organique Hétérocyclique, URAC 21, Pôle de Compétences Pharmacochimie, Université Mohammed V, Faculté des Sciences, Av. Ibn Battouta, Rabat, Morocco

²URAC18, COST, Laboratoire de Chimie Appliquée et environnement, Department of Chemistry, Faculty of Sciences, Mohamed 1st University, Oujda, Morocco

³Laboratoire de Chimie Organique Appliquée, Université Sidi Mohamed Ben Abdallah, Faculté des Sciences et Techniques, Route d'Immouzzar, Fès, Morocco

⁴LIMME, Faculté des sciences Dhar El Mehraz, Université Sidi Mohammed Ben Abdullah, USMBA., Atlas, Fes, Morocco

ABSTRACT

The inhibition effect of 3-methyl-4-(3-methylisoxazol-5-yl)isoxazol-5(2H)-one monohydrate (P1) on the corrosion of carbon steel in 1 M HCl was studied by weight loss, electrochemical impedance spectroscopy (EIS) techniques and potentiodynamic polarization methods. The results showed that isoxazole P1 was a good inhibitor in 1 M HCl and inhibition efficiency increases with isoxazole P1 concentration to attain 93% at 10-3M at 308 K. E(%) values obtained from various methods used are reasonably good agreement. The adsorption of isoxazole P1 obeyed the Langmuir adsorption isotherm. Polarization curves showed that isoxazole P1 acted as a mixed-type inhibitor in HCl. The effect of the temperature on the corrosion behavior with addition of 10-3M of the inhibitor was studied in the temperature range 313-343 K, and the thermodynamic parameters were determined and discussed. In addition, a quantum chemical study suggests isoxazole P1 inhibitor is structurally essential for the protection of metal surface

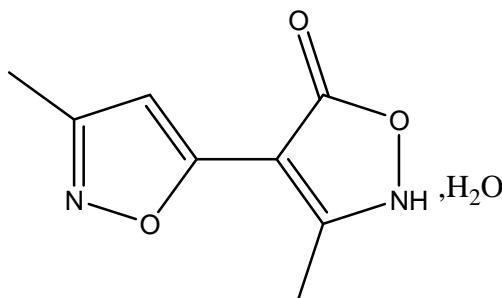
Key words: Mild Steel, EIS, Polarization, Weight loss, Acid inhibition, adsorption isotherm, DFT.

INTRODUCTION

Mild steel is widely used as structural material in engineering as well as daily life applications [1-5]. The study of corrosion inhibition of mild steel using organic inhibitors mainly in acidic media is one of the most important subjects of current research in different industries [6-10].

The role of inhibitors added in low concentrations to corrosive media is to decrease the dissolution of the metal with corrosive medium and is to inhibit the adsorption or coordination onto the metal surfaces [11, 12]. In our laboratory, many studies have been published on the use of natural products as corrosion inhibitors in acidic media [13-15]. Most of the effective organic inhibitors used contain hetero-atoms such as O, N, S and multiple bonds in their molecules through which they are adsorbed on the metal surface [16-18]. In general, the adsorption of an inhibitor on a metal surface depends on the nature and the surface charge of the metal, the adsorption mode, its chemical structure and the type of electrolyte solution [19]. Over the years, Isoxazole derivatives received much attention and found wide application in medicinal chemistry [20]. Generally, Isoxazole derivatives have found widespread application as fungicide and bactericide [21], antimicrobial agent in pharmaceuticals and cosmetics [22].

Subsequently performed EIS identified this compound as new corrosion inhibitor for mild steel in 1 M HCl with remarkably improved potency. Furthermore, gravimetric measurement, polarization, thermodynamic and DFT quantum chemical calculations were used to investigate in more detail the inhibitive characteristic of compound (P1) Scheme 1.



Scheme 1: 3-methyl-4-(3-methylisoxazol-5-yl)isoxazol-5(2H)-one monohydrate (P1). [23]

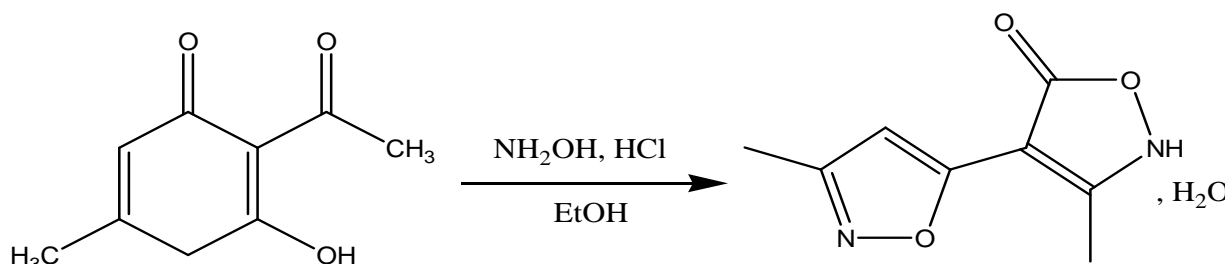
MATERIALS AND METHODS

2.1. Materials:

The mild steel strips having a composition (wt.%) of 0.09%P, 0.01 % Al, 0.38 % Si, 0.05 % Mn, 0.21 % C, 0.05 % S and Fe balance were mechanically cut into $1.5 \times 1.5 \times 0.05 \text{ cm}^3$ dimensions for the electrochemical experiments. The surface of the specimens was abraded with emery paper grade 600 and 1200, which was then washed in deionized water, degreased ultrasonically in ethanol and acetone. The acid solutions (1.0 M HCl) were prepared by dilution of analytical reagent-grade 98 % H₂SO₄ with double-distilled water. The range of concentration of isoxazole P1 was 10^{-6} M to 10^{-3} M.

2.2. Synthesis of inhibitors

A solution of 3-Acetyl-4-hydroxy-6-methyl-2H-pyran-2-one (1 g, 6 mmol) and an excess of hydroxyl-amine hydrochloride (1.25g, 18 mmol) in ethanol (30 mL) was stirred at room temperature for 24 hours. Completion of the reaction was confirmed by TLC. At the end of the reaction, the solution was concentrated and the solid was obtained by adding di-chloro-methane (CH₂Cl₂). The solid product was purified by recrystallization from ethanol to afford colourless crystals in 80% yield. Scheme 2.



Scheme 2: Characterization of 3-methyl-4-(3-methylisoxazol-5-yl)isoxazol-5(2H)-one monohydrate (P1)

The analytical and spectroscopic data are conforming to the structure of compound formed.

(P1): Yield = 80%; Spectre de RMN¹H (DMSO-d₆) δ ppm : 2.14 (s, 3H, CH₃); 2.25 (s, 3H, CH₃); 7.2 (s, 1H, CH); 6.14 (s, 1H, NH); Spectre RMN¹³C (DMSO-d₆) δ ppm : 13.1 (CH₃); 13.3 (CH₃); 105.75 (CH), 108.66 (Cq); 153.20 (Cq); 153.87 (Cq); 155.88 (Cq); 168.82 (C=O).

2.3. Measurements

2.3.1. Weight loss measurements

Gravimetric measurements are carried out in a double walled glass cell equipped with a thermostated cooling condenser. The solution volume is 100 cm³. The immersion time for the weight loss is 6 h at (308±1) K. Triplicate experiments were performed in each case and the mean value of the weight loss was calculated.

2.3.2. Electrochemical measurements

The electrochemical study was carried out using a potentiostat PGZ100 piloted by Voltmaster soft-ware. This potentiostat is connected to a cell with three electrode thermostats with double wall. A saturated calomel electrode (SCE) and platinum electrode were used as reference and auxiliary electrodes, respectively. Anodic and cathodic

potentiodynamic polarization curves were plotted at a polarization scan rate of 0.5mV/s. Before all experiments, the potential was stabilized at free potential during 30 min. The polarisation curves are obtained from -800 mV to -200 mV at 308 K. The solution test is there after de-aerated by bubbling nitrogen. The electrochemical impedance spectroscopy (EIS) measurements are carried out with the electrochemical system, which included a digital potentiostat model Voltalab PGZ100 computer at Ecorr after immersion in solution without bubbling. After the determination of steady-state current at a corrosion potential, sine wave voltage (10 mV) peak to peak, at frequencies between 100 kHz and 10 mHz are superimposed on the rest potential. Computer programs automatically controlled the measurements performed at rest potentials after 0.5 hour of exposure at 308 K. The impedance diagrams are given in the Nyquist representation. Experiments are repeated three times to ensure the reproducibility.

2.3.3. Quantum chemical study

The quantum chemical calculations were performed on an intel ® core™ i3 CPU (2,4 GHz, 4Go RAM) workstation.

Complete geometry optimizations of the undertaken 3-methyl-4-(3-methylisoxazol-5-yl)isoxazole-5(2H)-one as corrosion inhibitors were performed by using the density functional theory (DFT) [24], using the hybrid functional B3LYP taking into account exchange and correlation with Beck's three parameters exchange functional along with Lee-Yang-Parr [25]. Calculation at this level of theory DFT/B3LYP were done by using 6-31G(d,p) basis set implemented in Gaussian 09 package [26].

Theoretical studies were used to extend the gravimetric and electrochemical study on the corrosion inhibitors looking for good theoretical parameters to characterize their inhibition performance. Therefore, some molecular descriptors describing the global reactivity such as: E_{tot} , E_{HOMO} , E_{LUMO} , μ , electron affinity (A), the ionization potential (I), the electronegativity (χ), the fraction of electron transferred (ΔN).

RESULTS AND DISCUSSION

3.1. Weight loss measurements

The corrosion rate (W_{corr}) of mild steel coupons in 1 M HCl solution at different concentrations of **P1** was calculated using the following equation:

$$W_{corr} = \frac{m}{S \cdot t} \quad (1)$$

Where m is the weight loss of mild steel, S the total area of one mild steel, and t is immersion time. The obtained values of the gravimetric corrosion rates (W_{corr}) and the inhibition efficiency (E_w) are represented in Table 1. The inhibition efficiency $E_w\%$ corrosion in the case of this method was calculated from the following equation:

$$E(\%) = \left(1 - \frac{W'_{CORR}}{W_{CORR}}\right) \cdot 100 \quad (2)$$

Where W_{corr} and W'_{corr} are the corrosion rates of mild steel due to the dissolution in 1 M HCl in uninhibited and inhibited solutions, respectively. The results obtained from gravimetric measurements show for inhibitor tested that the corrosion rate values decrease when the concentration of isoxazole P1 increases. The analysis of **Table 1** show that protection efficiency degree of surface coverage increased with increasing concentration of inhibitor studied. This showed that isoxazole P1 in solution inhibited the corrosion of mild steel in 1 M HCl. The best action of this inhibitor is attained in the presence of $10^{-3}M$ of isoxazole P1.

Table 1. Corrosion parameters obtained from weight loss measurements for mild steel in 1 M HCl containing various concentrations of 3-methyl-4-(3-methylisoxazol-5-yl)isoxazol-5(2H)-one monohydrate (P1) at 308 K

Inhibitor	Concentration (M)	Wcorr (mg.cm ⁻² .h ⁻¹)	Ew (%)	θ
isoxazole P1	Blank	0.91	--	--
	10^{-3}	0.06	93	0.93
	10^{-4}	0.09	90	0.90
	10^{-5}	0.155	84	0.84
	10^{-6}	0.26	71	0.71

From the results, it was obvious that mild steel corroded in HCl solution. This is expressed in terms of weight loss of mild steel. Upon addition of inhibitor isoxazole P1, it was observed that the weight loss decreased as the corrosion rate and degree of surface coverage (θ). However, the weight loss decreased more as the concentration of inhibitor

increased.

3.2. Effect of temperature.

To assess the influence of temperature on corrosion and corrosion inhibition processes, gravimetric tests were carried out at various temperatures (313–343K) in the absence and presence of 10^{-3} M of isoxazole P1, as shown in Table 2.

Table 2. Inhibition efficiency and corrosion rates in the absence and presence of 10^{-3} M of isoxazole P1 at different temperatures after 60 min immersion

Temperature (K)	W _{corr} (mg.cm ⁻² .h ⁻¹)		θ	E _w (%)
	1M HCl	1M HCl + isoxazole P1		
313	1.51	0.21	0.87	86
323	3.21	0.72	0.77	77
333	6.53	2.03	0.68	68
343	10.12	4.20	0.58	58

Corresponding gravimetric data are given in Table 2. As seen from Table 2, the corrosion rates increases with increasing temperature, in both uninhibited and inhibited solutions. Inhibition efficiency for isoxazole P1 decreases with increase in temperature and a slight changes in there values are observed in the range of temperature studied. From this result, it can be concluded that the value of corrosion current density increases in the absence and the presence of inhibitor. After addition of the tested inhibitor in corrosive medium, the dissolution of mild steel is extensively retarded.

To calculate the activation parameters of the corrosion process, Arrhenius equation. (3) was used. [27]

$$W_{corr} = k \cdot \exp(-E_a/RT) \quad (3)$$

where k is the corrosion rate constant, E is the activation energy, T is the absolute temperature and R is the universal gas constant.

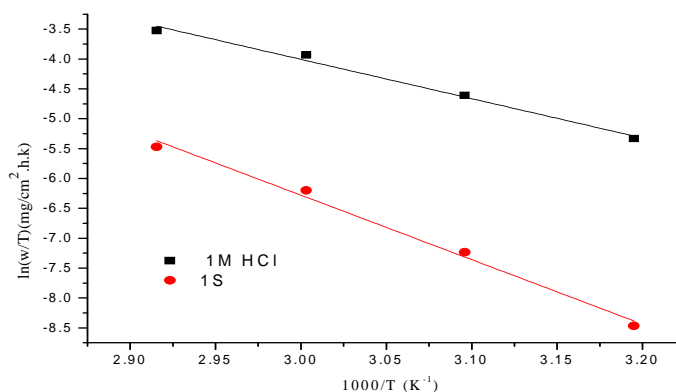


Figure 1. Arrhenius plots of mild steel in 1M HCl with and without 10^{-3} M of isoxazole P1

Figure 1 shows Arrhenius plots of the logarithm of the corrosion rates vs $1/T$ for mild steel in the corrosive medium with and without addition of 10^{-3} M of isoxazole P1. Straight lines are obtained with a slope of $(-E_a/R)$.

The value of E_a can be obtained from the slope of the straight line which was found to be $57.39 \text{ kJ} \cdot \text{mol}^{-1}$ and $89.65 \text{ kJ} \cdot \text{mol}^{-1}$ in the absence and presence of 10^{-3} M of isoxazole P1, respectively. The higher value of E_a in the presence of isoxazole P1 than its absence indicates a strong inhibitive action of the isoxazole P1 by increasing the energy barrier for the corrosion process [28-29]. And the higher E_a value in the inhibited solution can be correlated with the increased thickness of the double layer.

3.4. Adsorption isotherm

The mechanism of the interaction between inhibitor and the electrode surface can be explained using adsorption isotherms. Several adsorption isotherms were tested and the Langmuir adsorption isotherm was found to provide best description of the adsorption behavior of the investigated inhibitor. The Langmuir isotherm is based on the assumption that all adsorption sites are equivalent and that particle binding occurs independently from nearby sites, whether occupied or not. The degree of surface coverage (θ) for different concentrations of inhibitor in 1 M HCl has

been evaluated from weight loss measurements. The plot C_{inh}/θ against C_{inh} yields a straight line (Figure. 2), with correlation coefficient (R^2) values of 0.9999 for this inhibitor, at 308 K. This indicates that the adsorption of this inhibitor can be fitted to the Langmuir adsorption isotherm, represented by the equation [30]:

$$\frac{C}{\theta} = \frac{1}{k} + C \quad (4)$$

With

$$K = \frac{1}{55.55} \exp\left(-\frac{\Delta G_{\text{ads}}^0}{RT}\right) \quad (5)$$

Where C is the concentration of inhibitor, K is the adsorptive equilibrium constant, θ is the surface coverage and the standard adsorption free energy (ΔG_{ads}).

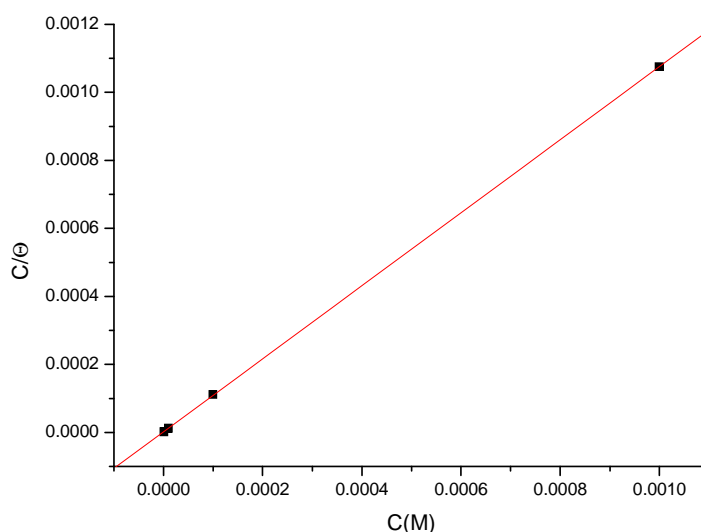


Figure 2. Langmuir adsorption of isoxazole P1 on the mild steel surface in 1 M HCl solution

The negative value of ΔG_{ads} ensure the spontaneity of the adsorption process and stability of the adsorbed layer on the metal surface. It is generally accepted that, for values of ΔG_{ads} up to -20 kJ/mol, the type of adsorption can be regarded as physisorption, in which case inhibition results from the electrostatic interactions between the charged molecules of the inhibitors and the charged metallic surface. In contrast, for values above -40 kJ/mol, the adsorption is regarded as chemisorptions, which is due to charge sharing or transfer from the inhibitor molecules to the metal surface to form a covalent bond [31]. The value of ΔG_{ads} in our measurement suggest that the adsorption of isoxazole P1 involves chemisorption.

Table 3. Thermodynamic parameters for the adsorption of isoxazole P1 in 1 M HCl on the mild steel at 308 K

Inhibitor	Slope	K_{ads} (M^{-1})	R^2	ΔG_{ads} (kJ/mol)
isoxazole P1	1.07	595869.43	0.9999	- 44.31

3.5. EIS studies

Nyquist plots for mild steel in 1 M HCl in the absence and presence of isoxazole P1 at various concentrations are shown in Figure 3. It was evident from these plots that the impedance response of mild steel in HCl has significantly altered after the addition of isoxazole P1 into the test solution. The plots were similar for different concentrations of isoxazole P1. Semicircles are obtained which cut the real axis at higher and lower frequencies. At higher frequency end, the intercept corresponds to R_s and at lower frequency end the intercept corresponds to $R_s + R_t$. The difference between these two values gives R_t .

Inhibition efficiency ($E_{R_t}\%$) is estimated using the equation 6, where $R_{t(0)}$ and $R_{t(\text{inh})}$ are the charge transfer resistance values in the absence and presence of inhibitor, respectively:

$$E_{R_t} \% = \frac{R_t(\text{inh}) - R_t(\text{e})}{R_t(\text{inh})} \times 100 \quad (6)$$

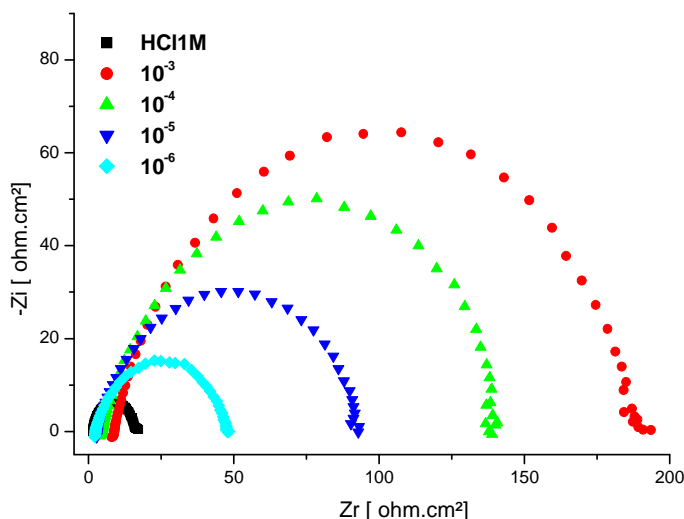


Figure 3. Nyquist plots for mild steel in 1 M HCl containing different concentrations of isoxazole P1

The results show that R_t values increased with increase of inhibitor concentration. The electrochemical impedance parameters derived from the Nyquist plots and the inhibitors efficiencies E_{R_t} (%) are shown in Table 4.

Table 4. AC impedance data of mild steel in 1.0 M HCl acid solution containing different concentrations of isoxazole P1 at 308K

Inhibitor	Concentration (M)	R_t ($\Omega \cdot \text{cm}^2$)	Cdl ($\mu\text{f}/\text{cm}^2$)	E_{R_t} (%)
HCl 1M	1M	14.7	200	--
isoxazole P1	10^{-3}	181	70	92
	10^{-4}	137	58	89
	10^{-5}	91	71	83
	10^{-6}	45	87	67

The results obtained from (EIS) method can be interpreted in terms of the equivalent circuit of the electrical double layer shown in Figure 4 which has been used previously to model the mild steel/acid interface [32]. The Nyquist plots were similar for different concentrations of isoxazole P1. The semicircle in all cases corresponds to a capacitive loop. The semicircle radii depend on the inhibitor concentration. The diameter of the capacitive loop increased with increase of inhibitor concentration.

From the Table 4, it was clear that charge transfer resistance values were increased and the capacitance values decreased with increasing inhibitor concentration. Decrease in the capacitance, which can result from a decrease in local dielectric constant and/or an increase in the thickness of the electrical double layer, suggests that the inhibitor molecules act by adsorption at the metal/solution interface [33]. This indicated the formation of a surface film on the mild steel.

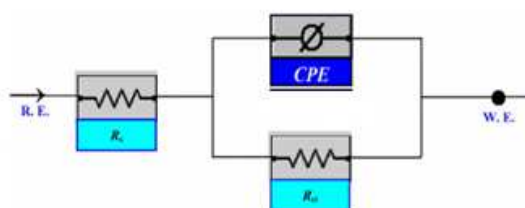


Figure 4. Equivalent circuit used to fit the EIS data of mild steel in 1M HCl at different concentrations of isoxazole P1

3.6 Polarization Measurements

Polarization curves for mild steel in 1M HCl in the absence and presence of isoxazole P1 at different concentrations at 308K are presented in Figure 5. The extrapolation of Tafel straight line allows the calculation of the corrosion

current density (I_{corr}). The values of I_{corr} , the corrosion potential (E_{corr}), cathodic Tafel slopes (β_c), and inhibition efficiency (E_p %) are given in Table 5. The inhibition efficiency is calculated using the following equation:

$$E_p \% = \frac{I_{\text{corr}(0)} - I_{\text{corr}(\text{inh})}}{I_{\text{corr}(0)}} \times 100 \quad (7)$$

where $I_{\text{corr}(0)}$ and I_{corr} are current density in absence and presence of isoxazole P1, respectively.

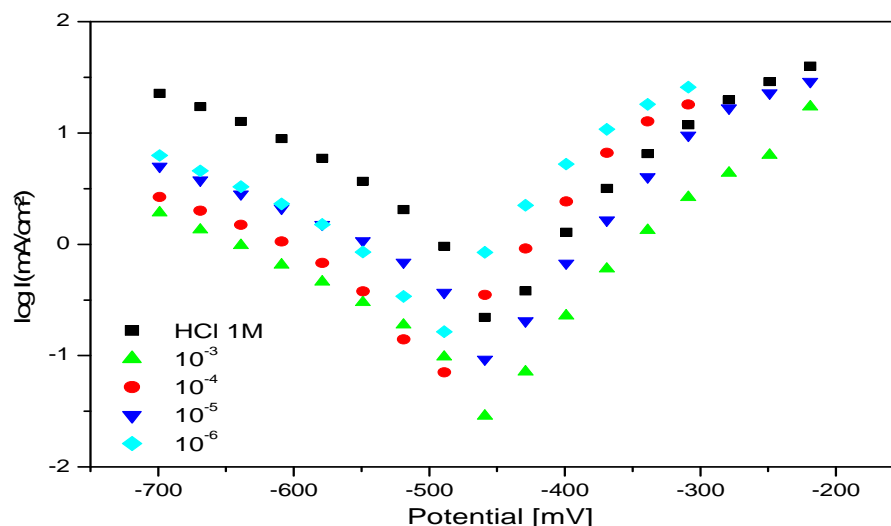


Figure 5. Potentiodynamic polarization curves of mild steel in 1M HCl in the presence of different concentrations of isoxazole P1

The values of I_{corr} decreased in the presence of inhibitor indicating that component of isoxazole P1 adsorb on the mild steel surface. The isoxazole P1 acted both on the cathodic and anodic branches. This result indicates that inhibitor acts as a mixed-type inhibitor. E_{corr} varies slightly in the inhibited and uninhibited solution; indicate that adsorption occurs by geometric blockage [34]. We also remark that the cathodic current–potential curves give rise to Tafel lines, which indicate that hydrogen evolution reaction is activation controlled. The values of the β_c show slight changes with the addition of isoxazole P1. This result means that the mechanism at the electrode reaction is not affected [35].

Table 5. Electrochemical parameters of mild steel in 1M HCl solution without and with isoxazole P1 at different concentrations

Inhibitors	Concentration (M)	E_{corr} (mV/SCE)	I_{corr} ($\mu\text{A}/\text{cm}^2$)	β_c	E_p (%)
HCl 1M	---	-459	1386	-294	--
isoxazole P1	10^{-3}	-433	97	-91	93
	10^{-4}	-433	123	-212	91
	10^{-5}	-455	401	-220	71
	10^{-6}	-457	566	-181	59

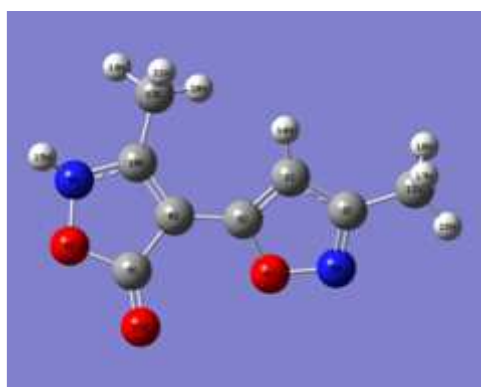


Figure 6: the optimized geometrical of 3-methyl-4-(3methylisoxazol-5-yl)isoxazole-5(2H)-one (P1) calculated at B3LYP/6-31G(d,p)

3.7. Quantum chemical calculations

The geometry of the molecule under investigation is determined by optimizing all structural parameters at B3LYP/6-31G(d,p) level of theory. The geometry is presented in figure 6, the bond length and bond angle are shown in table 6.

Table (6): selected bond length and dihedrals angles giving for 3-methyl-4-(3methylisoxazol-5-yl)isoxazole-5(2H)-one (P1) calculated at B3LYP/6-31G(d,p) level theory

Length bond	Value (Å°)
C ₁ —C ₂	1,42
C ₁ —C ₅	1,37
C ₂ —N ₃	1,31
C ₅ —O ₄	1,35
O ₃ —N ₃	1,39
C ₁₀ —N ₉	1,38
N ₉ —O ₈	1,40
C ₇ —O ₁₂	1,20
C ₅ —C ₆	1,44
Angle band	Value (d°)
C ₂ C ₁ C ₅	104,20
C ₂ N ₃ O ₄	105,97
C ₅ O ₄ N ₃	109,28
C ₁ C ₅ C ₆	133,27
C ₁₀ N ₉ O ₈	108,52
O ₈ C ₇ O ₁₂	120,28
C ₆ C ₇ O ₈	105,84
C ₅ C ₇ O ₁₂	133,87
Dihedrals angles	Value (d°)
N ₃ O ₄ C ₅ C ₆	179,48
C ₅ C ₆ C ₇ O ₈	-179,99
N ₉ C ₁₀ C ₆ C ₅	175,13
O ₁₂ C ₇ C ₆ C ₁₀	-179,24

The analysis of the theoretical results obtained, we can say that the molecule have a planar structure. The C₂—N₃ single bond lengths (1,31 Å) indicating the existence of a double bond. Moreover, the C₁₀—N₉ single bond lengths (1,38 Å) are shorter than typical carbon nitrogen single bond indicating of strong π electron delocalization in the ring who have C=O.

Global molecular reactivity

The global molecular reactivity can be studied according to Fukui's theory of frontier molecular orbital in terms of interaction between the frontier orbital, namely the HOMO and the LUMO [36]. The calculated energies of the frontier orbital presented in table 7:

Table 7: theoretical descriptors of the studied inhibitors calculated at B3LYP/6-31G(d,p)

Molecule	E _t (eV)	E _{HOMO} (eV)	E _{LUMO} (eV)	ΔE (eV)	μ (D)
isoxazole P1	-644,76	-6,26	1,16	7,42	8,37

Energy HOMO describe the electron donating ability of the molecule, conversely, energy LUMO describe the electron accepting ability of the molecule. The gap energy defined by ($\Delta E = E_{LUMO} - E_{HOMO}$), indeed, large value of the gap ($\Delta E = 7,42$) imply high electronic stability and then low reactivity.

The dipole moment μ explain the information on the polarity of the whole molecule. High dipole moment is reflected in important molecular polarity which probably gives rise to high chemical reactivity. In our case, we have a dipole moment value ($\mu = 8,37$) which implies that there leading to stranger adsorption on to the mild steel surface.

According to Lukovits et al [37] study, the fraction of electron transferred is giving by the expression:

$$\Delta N = \frac{\chi(Fe) - \chi(inhib)}{2[\eta(Fe) + \eta(inhib)]}$$

$$\Delta N = \frac{\chi(Fe) - \chi(inhib)}{2[\eta(Fe) + \eta(inhib)]} = 0,64$$

If $\Delta N < 3,6$ which indicates the tendency of a molecule to donate electrons to the mild steel surface.

CONCLUSION

From the principal result of the present work we can conclude that:

- The 3-methyl-4-(3-methylisoxazol-5-yl)isoxazol-5(2H)-one monohydrate (**P1**) was found to perform in 1 M HCl.
- Polarization study showed that the compound under investigation was mixed type inhibitor.
- The inhibition efficiency of the isoxazole P1 increased with the concentration and reached **93** % at 10^{-3} M.
- The weight loss, polarization curves and electrochemical impedance spectroscopy were in good agreement.
- The inhibition efficiency decreased with increasing temperature and their addition led to an increase of the activation corrosion energy.
- Adsorption of the inhibitor on the mild steel surface from 1 M HCl followed the Langmuir isotherm.
- The quantum mechanical approach may well be able to foretell molecule structures that are better for corrosion inhibition.

REFERENCES

- [1] H. Elmsellem, A. Elyoussfi, N. K. Sebbar, A. Dafali, K. Cherrak, H. Steli, E. M. Essassi, A. Aouniti and B. Hammouti, *Maghr. J. Pure & Appl. Sci*, **2015**, 1, 1-10.
- [2] A. Elyoussfi, H. Elmsellem, A. Dafali, K. Cherrak, N. K. Sebbar, A. Zarrouk, E. M. Essassi, A. Aouniti, B. El Mahi and B. Hammouti, *Der Pharma Chemica*, **2015**, 7(10), 284-291.
- [3] I. El Mounsi, H. Elmsellem, A. Aouniti, H. Bendaha, M. Mimouni, T. Benhadda, R. Mouhoub, B. El Mahi, A. Salhi and B. Hammouti. *Der Pharma Chemica*, **2015**, 7(10), 350-356.
- [4] F. Yousfi, M. El Azzouzi, M. Ramdani, H. Elmsellem, A. Aouniti, N. Saidi, B. El Mahi, A. Chetouani and B. Hammouti, *Der Pharma Chemica*, **2015**, 7(7),377-388.
- [5] M. Ramdani, H. Elmsellem, N. Elkhiati, B. Haloui, A. Aouniti, M. Ramdani, Z. Ghazi, A. Chetouani and B. Hammouti, *Der Pharma Chemica*, **2015**, 7(2),67-76.
- [6] N. Saidi, H. Elmsellem, M. Ramdani, A. Chetouani, K. Azzaoui, F. Yousfi, A. Aounitia and B. Hammouti, *Der PharmaChemica*, **2015**, 7(5),87-94.
- [7] H. Elmsellem, H. Bendaha, A. Aouniti, A. Chetouani, M. Mimouni, A. Bouyanzer, *Mor. J. Chem*, **2014**, 2 (1), 1-9.
- [8] I. El Mounsi, H. Elmsellem, A. Aouniti, H. Bendaha, M. Mimouni, T. Benhadda, R. Mouhoub, B. El Mahi, A. Salhi and B. Hammouti, *Der Pharma Chemica*, **2015**, 7(10),350-356.
- [9] F.Aouinti, H.Elmsellem, A.Bachiri, M.L.Fauconnier, A.Chetouani, b.Chaouki, A.Aouniti, B.Hammouti, *Journal of Chemical and Pharmaceutical Research*, **2014**, 6(7),10-23.
- [10] Y. EL Ouadi, A. Bouratoua, A. Bouyanzer, Z. Kabouche, R. Touzani, H. Elmsellem, B. Hammouti and A. Chetouani, *Der Pharma Chemica*, **2015**, 7(2):103-111.
- [11] I. El Mounsi, H. Elmsellem, A. Aouniti, H. Bendaha, M. Mimouni, T. Ben Hadd, H. Steli, M. Elazzouzi, Y. EL Ouadi and B. Hammouti, *Der PharmaChemica*, **2015**, 7(5):99-105.
- [12] M. El Azzouzi, A. Aouniti, L. Herrag, A. Chetouani, H. Elmsellem and B. Hammouti, *Der Pharma Chemica*, **2015**, 7(2):12-24.
- [13] Z. Ghazi, H. Elmsellem, M. Ramdani, A.Chetouani, R. Rmil, A. Aouniti, C. Jama, B. Hammouti, *Journal of Chemical and Pharmaceutical Research*, **2014**, 6(7):1417-1425.
- [14] A. Popova, E. Sokolova, S. Raicheva, M. Christov, *Corros. Sci*, **2003**, 45, 33.
- [15] F. Bentiss, M. Lebrini, M. Lagrenée, *Corros. Sci*, **2005**, 47, 2915.
- [16] N.K.Sebbar, H.Elmsellem, M.Boudalia, S.lahmidi, A.Belleaouchou, A.Guenbour, E. M.Essassi, H.Steli, A.Aouniti, *J. Mater. Environ. Sci*, **2015**, 6 (11), 3034-3044.
- [17] M. Lagrenée, B. Mernari, M. Bouanis, M. Traisnel, F. Bentiss, *Corros. Sci*, **2002**, 44, 573.
- [18] A.D.Becke, *Chem. Phys*,**1993**, 98, 5648.
- [19] A.D.Becke, *Phys. Rev. A*, **1988**, 38, 3098.
- [20] Cosimelli, B., Simorini, F., Taliani, S., La Motta, C., Da Settimo, F., Severi, E., Greco, G., Novellino, E., Costa, B., Da Pozzo, E., Bendinelli, S. & Martini, C. *Eur. J. Med. Chem*, **2011**, 46, 4506-4520.
- [21] Miller, R., Abacherli, C., Said, A. & Jackson, B. Ketenes, *Wiley-VCH Verlag GmCHand Co.KGaA*, **2001**.
- [22] J. J Kabara, *J. Am. Oil Chim. Soc.*,**1984**, 61, 397-403.
- [23] S.Lahmidi, M.Benchidmi, E.M.Essassi, M.Saadi and L.E.Ammari, *J.Mar.Chim.Heterocycl*, **2014**, 13, 53-59.
- [24] H. Elmsellem, A. Aouniti, M.H. Yousoufi, H. Bendaha, T. Ben hadda, A. Chetouani, I.Warad, B. Hammou, *Phys. Chem. News*, **2013**, 70, 84-90.
- [25] A. D. Becke, *phys.Rev*, **1998**, 83, 3098.
- [26] H. Elmsellem, M. H.Yousouf, A. Aouniti, T. Ben Hadd, A. Chetouani, B. Hammouti. *Russian, Journal of Applied Chemistry*, **2014**, 87(6), 744–753
- [27] H. Elmsellem, H. Nacer, F. Halaimia, A. Aouniti, I. Lakehal, A. Chetouani, S. S. Al-Deyab, I. Warad, R. Touzani, B. Hammouti, *Int. J. Electrochem. Sci*, **2014**, 9, 5328 – 5351

- [28] H. Elmsellem, N. Basbas, A. Chetouani, A. Aouniti, S. Radi, M. Messali, B. Hammouti, *Portugaliae. Electrochimica. Acta*, **2014**, 2,77.
- [29] H. Elmsellem, A. Aouniti, Y. Toubi, H. Steli, M. Elazzouzi, S. Radi, B. Elmahi, Y. El_Ouadi, A. Chetouani, B. Hammouti, *Der Pharma Chemica*, **2015**, 7, 353-364
- [30] I. Langmuir, *J. Am. Chem. Soc.*, **1947**, 39, 1848. 10.1021/ja02254a006
- [31] H. Elmsellem, T. Harit, A. Aouniti, F. Malek, A. Riahi, A. Chetouani, and B. Hammouti. *Protection of Metals and Physical Chemistry of Surfaces*, **2015**, 51(5), 873–884
- [32] H.Elmsellem, A. Elyoussfi, N. K. Sebbar, A. Dafali, K. Cherrak, H. Steli, E. M. Essassi, A. Aouniti and B. Hammouti, *Maghr. J. Pure & Appl. Sci*, **2015**, 1, 1-10.
- [33] M.Boudalia, A.Bellaouchou, A.Guenbour, H.Bourazmi, M.Tabiyaoui, M.El Fal, Y.Ramli, E.M.Essassi, H.Elmsellem, *Mor. J. Chem*,**2014**, 2, 97.
- [34] H. Elmsellem, A. Aouniti, M. Khoutoul, A. Chetouani, B. Hammouti, N. Benchat, R.Touzani, M. Elazzouzi. *Journal of Chemical and Pharmaceutical Research*, **2014**, 6(4), 1216-1224.
- [35] A. Aouniti, H. Elmsellem, S. Tighadouini, M. Elazzouzi, S. Radi, A. Chetouani, B. Hammouti, A. Zarrouk, *Journal of Taibah University for Science*,**2015**, <http://dx.doi.org/10.1016/j.jtusci.2015.11.008>
- [36]H. Elmsellem, K. Karrouchi, A. Aouniti, B. Hammouti, S. Radi, J. Taoufik, M. Ansar, M. Dahmani, H. Steli and B. El Mahi, *Der Pharma Chemica*, **2015**, 7(10),237-245.
- [37] I. Lukovits, E. Kalman, F. Zucchi, *Corrosion*, **2001**,57,3-7.